Inferring Galaxy Morphology Through Texture Analysis

Oriented Fliters vs. Curvelets

Joseph Richards
Andrew Connolly

March 9, 2007

1 Introduction

Galaxies are enormous, gravitationally-bound collections of stars, inter-stellar gas and dust, and dark matter. They generally contain between 10^7 and 10^{12} stars. Galaxies are constantly changing through gravitational interactions with the gas, dust, and other galaxies in their local environment. These encounters cause galaxies to change significantly throughout their lifetimes. The result is a diverse collection of galaxy morphologies throughout the observable universe. Studying galactic morphologies can give astronomers insight into the subtleties of galactic interaction dynamics and can provide details of the long-term trends in galactic evolution.

Galaxies are generally classified into three main groups based on morphology: ellipticals (E's), spirals (S's), and irregulars (Irr's) (Figure 1). Spiral galaxies are further split into regular spirals (S's) and barred spirals (SB's). The main classes of galaxies are in turn divided into sub-groups based on either the ellipticity of E-type galaxies or the tightness of the spiral arms (curvature) of S-type galaxies. This galactic classification scheme was first proposed by Edwin Hubble in 1936 [9].

Hubble believed both that galaxies evolved morphologically in an isolated environment and that the overall trend in galactic evolution was from ellipticals to spirals. Modern theory, however, claims (with a great deal of supporting evidence) that galaxies evolve through gravitational interactions with their surrounding environment. Additionally, astronomers now believe that ellipitcal galaxies are the by-products of interactions between spiral galaxies, which are believed to dominate the early universe.

In an ongoing effort to quickly and precisely characterize the morphological types of potentially millions of galaxies, a collaboration led by astronomer Andrew Connolly (Google, formerly at University of Pittsburgh) has studied methods of texture analysis to extract important morphological features of galaxies. In doing so, the group wishes to answer two main research questions. First, how has the distribution of galactic morphologies in the universe changed with time? In other words, what is the general trend of galactic evolution in the universe? In Astronomy, the further away an object is from us, the earlier in its history we perceive it. Therefore, a deep survey of galaxies provides us an instantaneous snapshot of the entire timeline of galactic evolution in our universe. Secondly, how does the

local density of galaxies affect the distribution of morphological types? An answer to this question in turn answers the more scientifically interesting question of how galactic collisions affect galaxy morphology, since local density is a strong indicator of galactic collision rate.

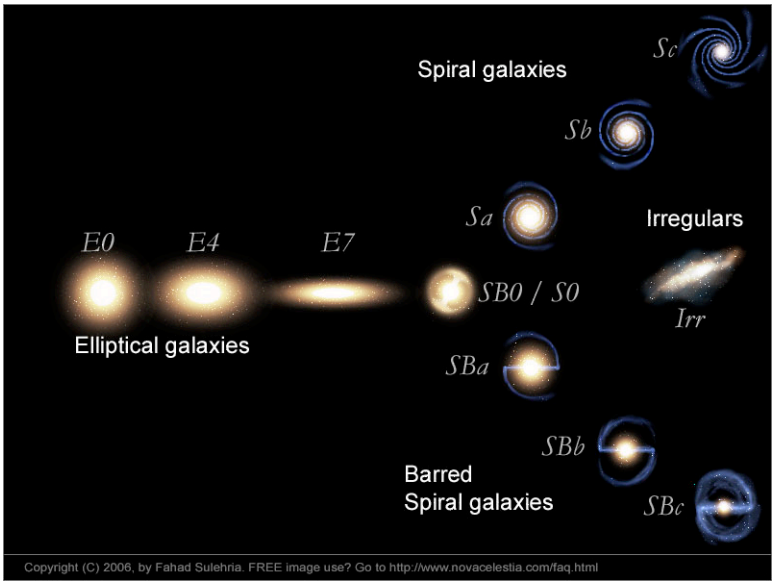

Figure 1: Galactic classification scheme devised by Hubble. The three main classes of galaxy morphology are ellipticals (E's), spirals (S's), and irregulars (Irr's). Spiral galaxies are divided into regular (S's) and barred (SB's) subtypes, and are further classified by the tightness of the spiral arms.

2 The Data

Modern sky surveys have the ability to gather data on millions of galaxies. This sheer amount of data, in the form of mega-pixel digital images, makes it impossible for astronomers to manually study these objects. The classical technique of studying galactic morphologies through visual image inspection is now infeasible. Therefore, we must devise methods that can quantitatively extract important morphological features from galactic images.

One survey in particular, the Sloan Digital Sky Survey (SDSS), promises to obtain images of millions of galaxies [11]. SDSS, when completed, will optically image over a quarter of the entire sky. In June 2005, SDSS completed its first phase, SDSS-I, a five-year campaign that returned data on more than 675,000 galaxies. Now SDSS is in its second phase, SDSS-II, which will last through June 2008.

Our purpose in this project is to compare methods that attempt to automatically extract important morphological features from digital galaxy images. We have at our disposal hundreds of galactic images with which to test these methods. Particularly, from SDSS-I

we have RC3, a sample of over 1400 galaxies in G, R, and I bands plus the corresponding composite images produced by combining the images from these three filters [8].

3 Methods

Our particular role in this project is to compare the ability of two different texture analysis methods (methods that look for local spatial structure) to extract the important morphological features of galaxies. We will compare the method of oriented filters employed by Au [1], who used the steerable pyramid algorithm of Simoncelli and Freeman [10] with the ridge function used by Candes and Donoho [5], with the methods of curvelet decomposition developed by a team led by Donoho [7, 3] in the ability to detect galaxy structures in digital images. Each of these techniques is a method of extracting the anisotropic features of image intensity, i.e. the axis-dependent properties of an image. For example, structures such as lines, curves, and edges have high anisotropicity and are captured by these techniques while point-like features have low anisotropicity and are ignored. We now briefly discuss the mathematical details of each of the two methods.

3.1 Oriented Filters

The oriented filter method for image analysis used by Au consists of two main steps [1]. First, it performs orientation analysis of texture for nine different angles on three different scales, and second, it merges the information elicited from these three scales to create a unified orientation field for the image (Figure 2).

At each section of an image, and at 9 different orientations, Au characterizes the strength of orientation by applying a 2D ridge function filter. The ridge function at position $\mathbf{x} = (x, y)^T$ and orientation angle θ is defined as

$$\rho_\theta(\mathbf{x}) = \frac{2}{\sqrt{3}}\pi^{-1/4}(1 - (\mathbf{x}^T r)^2)e^{-(\mathbf{x}^T r)^2/2} \tag{1}$$

where $r = (\cos(\theta), \sin(\theta))$. The function ρ_θ is designed for sparse approximation of linear singuarity in an image [5], and thus will yield high signal for directions θ that follow linear structures.

However, Equation (1) does not have localized support. To characterize only the local intensity structure at each location, Au applies a Gaussian window to ρ_θ,

$$\psi_\theta(\mathbf{x}) = \rho_\theta(\mathbf{x}) \times \frac{1}{\sqrt{2}}e^{-1/2(x^2+y^2)}. \tag{2}$$

Using this filtering scheme, Au defines the ψ discretized transform (DT^ψ) of a digital image I by

$$S_{\theta,\mathbf{x}} = (DT^\psi I)(\theta, \mathbf{x}) = I * \psi_\theta^D(\mathbf{x}), \tag{3}$$

i.e. the convolution of the image intensity with the discretized version of ψ_θ. Note that this transformation captures the isotropic features of an image for a single spatial scale. We

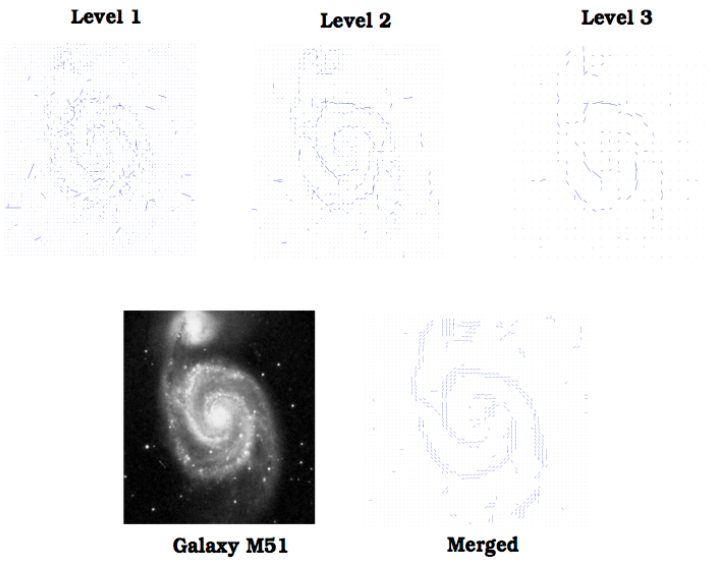

Figure 2: Application of oriented filters to galaxy M51. Orientation analysis is performed on three different spatial levels before being merged into one orientation field via Kalman filtering. The three levels here correspond to further subsampling of the lowpass subband.

can then estimate the orientation angle and strength at each point $\mathbf{x}$ in the image for this spatial scale by the vector $\mathbf{r}$, defined as

$$\mathbf{r}(\mathbf{x}) = \sum_{\theta} S^2_{\theta,\mathbf{x}} e^{2i\theta} \tag{4}$$

where $i = \sqrt{-1}$. In this manner, $\mathbf{r}$ is the sum of the signal energy vectors, and thus measures the concentration of signal energy under the filtering scheme and at which angle this energy concentrates most. The output of this technique when applied to a two-dimensional image is a 2-D orient vector field.

To capture anisotropic features on different spatial scales, Au employs the pyramid coding algorithm [10]. By applying the filter in Equation (2) for 9 different values of θ, we achieved angular localization in the Fourier plane. To analyze the texture on different spatial scales, we also need radial localization, which is achieved by first separating the original image into low and highpass subbands and then further passing the lowpass subband through the oriented filters described above. The resultant image is subsampled by a factor of 2 (thus keeping every second pixel in each dimension) to create a coarser representation of oriented image signal.

Au repeats this pyramid downsampling scheme down to three levels. The vector field is estimated for each subsampled image, and then the information from each level is recombined into a single orient vector field representation through Kalman filtering (See [2]). Again, refer to Figure 2 for an example of this implementation.

3.2 Curvelets

Curvelets were developed [12, 4, 3] to address the problem of sparse representation of objects with lines and edges. Conceptually, the 2-D curvelet transform is similar to the multiscale pyramid scheme mentioned above, with many directions and positions at each length scale and needle-shaped elements at fine scales. A distinguishing characteristic of the curvelet transform is its parabolic scaling relation that at each scale 2^{-j}, every individual element is contained in a ridge of length $2^{-j/2}$ and width 2^{-j}.

We define the continuous-time curvelet transform in $\mathbf{R}^2$ for spatial variable $\mathbf{x} = (x, y)$ at scale 2^{-j}, orientation θ_l, and position $\mathbf{x}_k^{(j,l)} = R_{\theta_l}^{-1}(k_1 \cdot 2^{-j}, k_2 \cdot 2^{-j/2})$ by

$$\varphi_{j,l,k}(\mathbf{x}) = \varphi_j \left(R_{\theta_l}(\mathbf{x} - \mathbf{x}_k^{(j,l)}) \right) \tag{5}$$

where φ_j is the Fourier transform in the domain at scale 2^{-j}, and $k = (k_1, k_2) \in \mathbf{Z}^2$ is a translation parameter.

With this definition, we can then define a curvelet coefficient of an image f at scale 2^{-j}, orientation θ_l, and translation k as the inner product between f and the curvelet $\varphi_{j,l,k}$ defined in Equation (5) as

$$c(j, l, k) = \langle f, \varphi_{j,l,k} \rangle = \int_{\mathbf{R}^2} f(\mathbf{x}) \overline{\varphi_{j,l,k}(\mathbf{x})} d\mathbf{x} \tag{6}$$

In practice, because we are using pixelated images, we employ a discretized version of the continuous curvelet transform, the digital curvelet transform. Details of two separate implementations of the digital curvelet transform can be found in [3]. Matlab implementation of this transform and its inverse transform are in the CurveLab package at http://www.curvelet.org.

After computing the curvelet coefficients, we reconstruct the image f from the m largest coefficients. This reconstruction, f_m leaves us the prominent anisotropic features of the original image and thresholds isotropic features such as point sources. The output, then, is a two-dimensional intensity field, as opposed to the 2-D vector field produced by orientation analysis. Moreover, the approximation error to the original image achieves

$$||f - f_m||_{L^2}^2 \leq C \cdot (\log m)^3 \cdot m^{-2} \tag{7}$$

for a curve that is C^2 except for discontinuities along C^2 curves.

4 Discussion

4.1 MatLab implementation of orientation analysis

For each of the two orientation analysis techniques, I use functions created in MatLab [1, 3]. The orientation analysis routines use MatLab functions from Simoncelli and Freeman [10] and a set of filters constructed by Au [1] (pp. 85-91) to extract the orientation fields on three different spatial scales and then combine them into a unified vector field. I apply the MatLab routines exactly as described by Au [1]. The output of these routines is a vector field akin to the merged image in Figure 2. Alternatively, we could extract and merge

information on more than 3 scales, but for now we will only consider the implementation of Au.

The curvelet MatLab routines consist of the digital curvelet and inverse digital curvelet transforms. After performing the digital curvelet transformation, I keep only a small proportion, m, of coefficients before transforming back into the original image space. The resultant image contains the prominent anisotropic features and thresholds the isotropic features, such as stars. In this technique we must also concern ourselves with the tuning parameter, m, whose value significantly changes the final intensity field (see Figure 3).

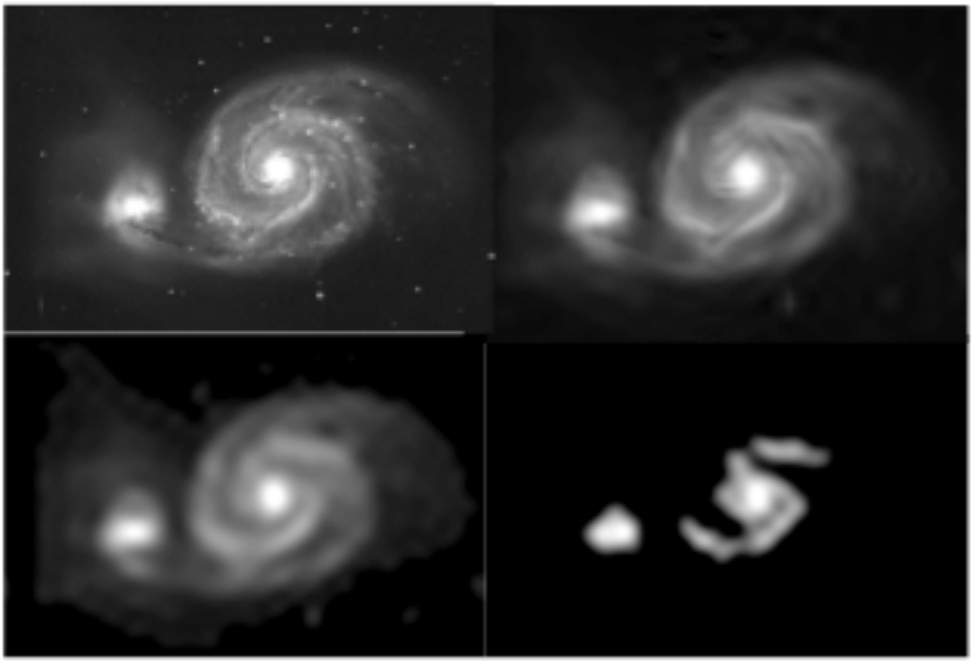

Figure 3: Original image of galaxy M51 plus three images produced by curvelet coefficient thresholding, in order of increasing threshold level (0.002, 0.001, and 0.0001 proportion of curvelet coefficients are used in the image reconstruction, respectively). Observe that isotropic features, such as foreground stars, are filtered by this technique. As more curvelet coefficients are cut, less fine details are observed, and the spiral arms are the prominent features. When too many coefficients are thresholded, the main structures of the galaxy are partially lost.

First-order comparisons of the two techniques have been performed with test images of galaxies M51, M63, M64, and M65. All of these are large spiral galaxies. The images were taken from http://www.seds.org/messier/. From these images, we find that both techniques seem to fare similarly in extracting the spiral features of the galaxies for images with differing quality and size. One difficulty in the curvelet method is that the tuning parameter, m, has a different optimal value in different images (optimality being defined as the threshold level that eliminates foreground stars but keeps the spiral structure intact).

This is an issue that will be better solved when we start model fitting.

4.2 Further Work

The next step in this project is to apply these two methods to the spiral head-on galaxies in the SDSS RC3 survey and then fit parametric physical spiral arm models to the output of each method. The RC3 survey consists of 105 galaxies that are both spiral and are oriented perpendicular to our line of sight. We do not necessarily need to restrict our attention to galaxies that are perpendicular to our line of sight, but doing so allows us to fit a simpler model that does not include galaxy inclination as a parameter.

For each of the 105 galaxies in our dataset we have determined both the Hubble and the de Vaucouleurs classification (a more finely-divided modification of the Hubble scheme [6]). Because we have already restricted our attention to spiral galaxies, we are concerned only with the amount of curvature in the spiral arms, which is accounted for in both the Hubble and de Vaucouleurs classification systems. If we can estimate the amount of curvature of the spiral arms of these galaxies from the outputs of both the oriented filters and curvelet techniques, we can then directly compare these values to the predicted curvature due to the galaxy's classification. This gives us a method of directly determining which method more accurately extracts galaxy arm features.

To determine the curvature of galaxy arms from the oriented filter output (a vector field) or curvelet reconstruction (an intensity field) we will fit the following logarithmic spiral arm model in polar coordinates

$$\theta = t + k \tag{8}$$

$$r = \beta e^{\alpha t},\ 0 \leq t \leq T, \alpha \leq 0, \tag{9}$$

where k, β are the initial angle and radial length, T is the winding angle of the spiral arm, and α controls the curvature of the spiral (a smaller α means higher curvature) [1]. To fit the curve, we need to determine an appropriate objective function to minimize for both a vector and intensity field. The optimal curvelet tuning parameter m may also be determined during this model fitting process.

Once we fit the model in Equation (8), we can quantify the integrated curvature of the galaxy, C, by

$$C = \int_0^T \frac{e^{-\alpha t}}{\beta\sqrt{1+\alpha^2}} dt = \frac{1 - e^{-\alpha T}}{\alpha\beta\sqrt{1+\alpha^2}} \tag{10}$$

If we determine the value of C for each of the 105 head-on spiral galaxies, we should be able to determine which technique, if either, is superior in extracting the spiral features of galaxies.

This should give us insight into our longer term goal of determining which technique should be implemented to the potentially millions of galactic images that will be captured by the Sloan Digital Sky Survey to automatically detect isotropic features and classify the galaxy accordingly.

References

[1] Kinman Au. *Inferring Galaxy Morphology Through Texture Analysis*. PhD thesis, Carnegie Mellon University, 2006.

[2] Peter J. Brockwell and Richard A. Davis. *Time Series: Theory and Methods*, page 37. Springer, 2nd edition, 2006.

[3] Emmanuel Candes, Laurent Denmanet, David Donoho, and Lexing Ying. Fast discrete curvelet transforms. *Multiscale Modeling and Simulation*, 5(3):861–899, 2006.

[4] Emmanuel Candes and David Donoho. New tight frames of curvelets and optimal representations of objects with c^2 singularities. *Comm. Pure Appl. Math.*, 57:219–266, 2002.

[5] Emmanuel J. Candes and David L. Donoho. Ridgelets: a key to higher-dimensional intermittency? *Phil. Trans. R. Soc. Lond. A*, 1999.

[6] G. de Vaucouleurs and A. de Vaucouleurs. Reference catalogue of bright galaxies, 1964.

[7] David L. Donoho and Mark R. Duncan. *Digital Curvelet Transform: Strategy, Implementation and Experiments*, November 1999.

[8] David W. Hogg and Michael R. Blanton. Sdss images of selected rc3 galaxies.

[9] E.P. Hubble. *The realm of the nebulae*. Yale University Press, 1936.

[10] Eero P. Simoncelli and William T. Freeman. The steerable pyramid: A flexible architecture for multi-scale derivative computation. In *2nd IEEE International Conference on Image Processing*, volume III, pages 444–447, October 1995.

[11] Sloan digital sky survey (sdss).

[12] J.L. Starck, D.L. Donoho, and E.J. Candes. Astronomical image representation by the curvelet transform. *Astronomy & Astrophysics*, 2002.